# Determination of Temperatures Using CH Radical Emission Spectroscopy



2012 Chinese Phys. Lett. 29 104707

(http://iopscience.iop.org/0256-307X/29/10/104707)

CHIN. PHYS. LETT. Vol. 29, No. 10 (2012) 104707

# Determination of Temperatures Using CH Radical Emission Spectroscopy *

YANG Qian-Suo(杨乾锁)**, SONG Jun-Hao(宋军浩), ZHU Nai-Yi(竺乃宜)

*State Key Laboratory of High Temperature Gas Dynamics, Institute of Mechanics, Chinese Academy of Sciences, Beijing 100190*

(Received 16 July 2012)

*An improved Boltzmann plot method where the intensity is taken as the integral of the experimental spectrum within a special band for a cluster of a rotational line of R and Q branches is proposed. This method aims at deducing rotational and vibrational temperatures using CH radical $A^2\Delta\rightarrow X^2\Pi$ band emission spectroscopy accurately. In addition, the data relative to the rotation lines of CH ($A^2\Delta\rightarrow X^2\Pi$) for both temperatures are assembled. The emission spectrum of CH ($A^2\Delta\rightarrow X^2\Pi$) at the inner cone of an acetylene-oxygen flame in a rich oxygen state is recorded and both of the temperatures are determined by the above-mentioned method. The values are recorded as 3141 K and 3097 K, for the rotational and vibrational temperatures, respectively. This result reveals that the equilibrium between the rotation and vibration states is achieved. A simple discussion for this method is also provided.*

*PACS: 47.11.Kb, 07.60.Rd, 02.70.Hm, 32.70.Fw* DOI: 10.1088/0256-307X/29/10/104707

It is well known that the dissociation of hydrocarbon results in the accumulation of CH radicals in some environments with a high temperature, such as in a combustion and plasma system. From the view point of the CH radicals, rarefied arc-jet plasma can be utilised to simulate the atmospheric re-entry plasma formed around the surface of a spacecraft during its re-entry into the atmosphere of some astronomical bodies. This is due to the fact that the CH radicals at these ground test facilities also appear in the corresponding atmospheric re-entry plasma if there is a certain amount of methane in their atmosphere. In addition, using the emission spectrum of CH, some parameters of the plasma can be non-intrusively estimated.[1−7] For example, the values of the rotational temperature $T_{\rm r}$ and vibrational temperature $T_{\rm v}$ can be determined using the emission spectrum of $A^2\Delta\rightarrow X^2\Pi$ transition of the CH emission,[1−5] based on the theory that the equilibrium distributions of both the rotation and vibration distributions of the electronically excited CH satisfy the Boltzmann distribution law.

In recent years, the experimental spectrum (ES) of CH ($A^2\Delta\rightarrow X^2\Pi$) obtained using spectrometers with a high wavelength resolution has been used to determine $T_{\rm r}$ of CH. In these experiments, the lines of $R$ branch in the ground vibration band for $T_{\rm r}$ are well separated from the neighbouring lines in ES and, therefore, their intensities are taken as the heights of the corresponding spectral peaks.[1,2,4] The accuracy of the measurement using this method has been validated by the line reversal method.[2,8,9] After having the intensities, $T_{\rm r}$ can also be determined by the optimal fittings of ES with the numerical spectrum (NS).[3−6,10] Finally, it is considered that $T_{\rm r}$ is equal to the translational temperature because a sufficiently fast relaxation usually exists between rotational states and translational states.[4,11,12]

However, the heights of the rotational lines are not always linearly proportional to the corresponding intensities and the accuracy of the temperature rapidly decreases with the resolution of the spectrometer, which can become so low that these rotational lines overlap with the other lines. In addition, the accuracy of $T_{\rm r}$ decreases with the increasing difference between the optical apparatus functions (OAF) of NS and those of ES because OAF of ES is not usually a theoretical formula. Therefore, it is not easy to determine $T_{\rm r}$ by fitting ES from an NS for $T_{\rm r}$ with a high accuracy.

In this Letter, an improved Boltzmann plot method is proposed for determining $T_{\rm r}$ and $T_{\rm v}$ by using ES from $A^2\Delta(0,N')\rightarrow X^2\Pi(0,N'')$ with a low wavelength resolution, based on the fact that the $Q$ branch of $A^2\Delta(2,N')\rightarrow X^2\Pi(2,N'')$ has a distinctive characteristic of having a very narrow wavelength distribution range. Thus, there is a peak for $T_{\rm v}$ in the corresponding spectral profile.[1,2,4] The vibrational temperature is also determined by combining some lines of $R$ branch in the $A^2\Delta(0,N')\rightarrow X^2\Pi(0,N'')$ where the intensities are equal to the integrals of the lines within broadening ranges. By using the ES from the inner core of an acetylene-oxygen flame in an oxygen-rich atmosphere, $T_{\rm r}$ and $T_{\rm v}$ are determined and the measured result reveals that $T_{\rm v}$ is approximately equal to $T_{\rm r}$.

The species at different rotational levels satisfy the Boltzmann distribution law at the thermal equilibrium state. Therefore, the intensities of the rotational lines in the emission spectrum can be used to determine $T_{\rm r}$. The equation characterising each rotational line of the emission of $A^2\Delta(\nu',N')\rightarrow X^2\Pi(\nu'',N'')$ is written as[1,2,4,5,13,14]

$$I_i = CA_{v'}S_i\nu_i^4\exp(-E_{v'N'i}/kT_{\rm r})\exp(-E_{v'i}/kT_{\rm v}), \quad (1)$$

where $A_{v'}$, $S_i$, and $\nu_i$ is the transition probability of the vibration state, the Hönl–London factor, and the

*Supported by the National Natural Science Foundation of China under Grant No 10472123.

**Corresponding author. Email: qsyang@imech.ac.cn

wave number of the $i$th rotational line. $E_{v'i}$ and $E_{v'N'i}$ are the upper levels of the corresponding vibration state and those of the rotation state for this line, respectively; $k$ and $C$ are the Boltzmann constant and a constant for the spectral intensity, respectively.

The data of the emission spectrum of the diatomic molecules[13] show that the intensities of the rotational lines with $\nu' = \nu''$ are much stronger than those with $\nu' \neq \nu''$ due to the fact of $A_{v'}(v' = v'') \gg A_{v'}(v' \neq v'')$. Therefore, the spectral intensity profile is made up mainly from the rotation lines with $\nu' = \nu''$. $I_i$ can be measured from the ES; $A_{v'}$, $S_i$, $\nu_i$, $E_{v'N'i}$ and $E_{v'i}$ are all known, thus, three unknown variables $C$, $T_\mathrm{r}$ and $T_\mathrm{v}$ are noted in Eq. (1). $T_\mathrm{r}$ can be uniquely determined by two rotational lines if the rotation lines both are chosen from one vibration band. More lines in the emission spectrum are used in the Boltzmann plot method to improve the accuracy of $T_\mathrm{r}$.[1,2,4] Moreover, if the peaks of these rotational lines are isolated from the neighbouring lines, their heights are linearly proportional to their intensities. The wavelength resolution of the spectrometer should be higher than 0.05 nm, considering that the wavelength intervals of the neighbouring rotational lines are from about 0.01 to 0.1 nm.[13] Unfortunately, the signal-to-noise ratio of an ES usually deteriorates with the increasing wavelength resolution of a special spectrometer.

In an ES, a rotational line is convoluted into a band with a certain profile. Moreover, the wavelength resolution of the spectrometer decreases to a state, which is so low that the band of a rotational line may overlap with the neighbouring lines. Thus, its intensity is not represented by its height. However, in an isolated spectral band with a zero value at the two edges $\lambda_1$ and $\lambda_2$, the intensity is the sum of the convolutions of $N$ rotational lines, Eq. (1) is developed into

$$\int_{\lambda_1}^{\lambda_2} I(\lambda)d\lambda = C\sum_{i}^{N} A_{v'}S_i\nu_i^4 \exp(-E_{v'N'i}/kT_\mathrm{r}) \cdot \exp(-E_{v'i}/kT_\mathrm{v}). \quad (2)$$

The more the intensities at the two sides of an isolated band approach the zero value, the higher the accuracy of Eq. (2) for an ES. Several rotational lines of the $R$ branch of the $A^2\Delta(0, N')\rightarrow X^2\Pi(0, N'')$ are chosen to speculate $T_\mathrm{r}$ in the process of determining $T_\mathrm{r}$. $T_\nu$ is then calculated using the intensity integral of some lines of the $Q$ branch of the $A^2\Delta(2, N')\rightarrow X^2\Pi(2, N'')$ with a known $T_\mathrm{r}$.

The emission of CH ($A^2\Delta\rightarrow X^2\Pi$) comes from the electronic transition between the $A^2\Delta$ and the $X^2\Pi$ states. The upper level $E_{v'N'}$ is split into four levels. Thus, every vibrational transition consists of 12 main branches and 12 satellite branches. The radiation from the main branches is much stronger than that from the satellite branches[13] and the wavelength ranges from 414 nm to 441 nm.[1,2,4,5,13] Figure 1 shows the wavelength distribution and Hönl–London factors of the main branches of $\nu'' = 0$, $\nu'' = 1$, and $\nu'' = 2$, where their wavelengths of four $R$ branches decrease with increasing $N''$ and the rotational lines with $\nu'' = 0$ overlapped with those with $\nu'' = 1$ and $\nu'' = 2$. However, the $Q$ branch with $\nu'' = 2$ is away from $Q$ branches with $\nu'' = 0$ and $\nu'' = 1$ and appears as an isolated peak in the ES.[1,2,4,5] On the other hand, Hönl–London factors of the main branches all increase with $N''$. However, the values of Hönl–London factor of the lines in satellite branches decreases versus $N''$ and their maximum is also smaller than the minimum of Hönl–London factors of the main branches. Therefore, the contributions of the satellite branches to the spectral distribution can be ignored.

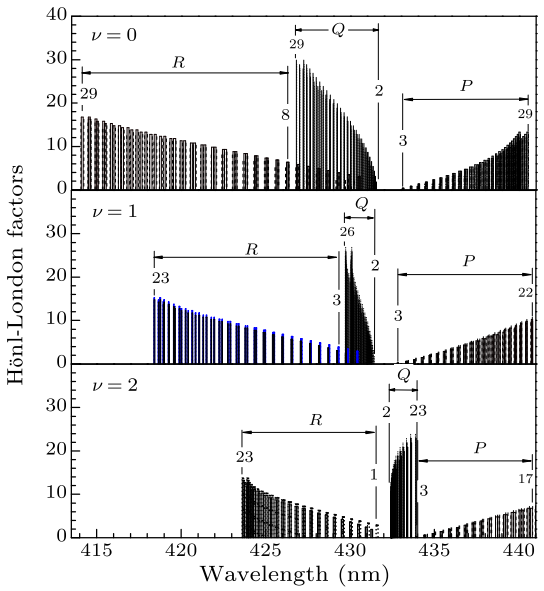


**Fig. 1.** Wavelength distribution and Hönl-London factors of the main branches of CH ($A^2\Delta\rightarrow X^2\Pi$).

The method described above is utilised to initially determine $T_\mathrm{r}$, where the intensities of the rotational lines are taken as the integral of the spectral intensity at the corresponding isolated bands. The parameters of $R$ branches with $N''$ from 13 to 19 and $\nu'' = 0$ are listed in Table 1. The values of the Hönl–London factors of the lines of $\nu_{1eRN''}$ and $\nu_{2eRN''}$ are equal to each other, $S_{0eN''}$. Hönl–London factors of $\nu_{1fRN''}$ and $\nu_{2fRN''}$ are also equal to one value of $S_{0fN''}$. Since the differences of the upper levels of the four lines all are at the 0.1 $\mathrm{cm}^{-1}$ level, Eq. (2) for the $R$ branch containing the four rotational lines is degenerated into

$$\int_{N''} Id\lambda = C[S_{0eN''}(\nu_{1eRN''}^4 + \nu_{2eRN''}^4) + S_{0fN''}(\nu_{1fRN''}^4 + \nu_{2fRN''}^4)]e^{-E_{0N''}/kT_\mathrm{r}} \cdot A_{v''}e^{-E_0/kT_\mathrm{v}}, \quad (3)$$

where $E_{0N''}^e + E_{0N''}^f = 2E_{0N''}$, as shown in Table 1.

To determine $T_\mathrm{r}$ of the inner core of an acetylene oxygen flame under a rich oxygen condition, the ES of OH and CH in this region are recorded. Figure 2 shows the recorded spectrum where the wavelength resolution of the spectrometer used is 0.09 nm, the pressures of oxygen and acetylene are all 0.4 MPa, and

the flux of oxygen is about 4–5 times compared to that of acetylene. Figure 2(a) shows that a typical spectral peak from the main branches of CH (C–$X$) for $\nu'' = 0$ is located at 314.2 nm, which represents the existence of CH radicals.[16] Apart from the inner core, the intensity of this peak rapidly weakens, thus the density of CH also declines. Figure 2(b) represents the corresponding ES at the inner core of the flame.

**Table 1.** Parameters of the rotational lines of the $R$ branch with $\nu'' = 0$.[13,14]

| $N''$ | $E^e_{0N''}$ | $E^f_{0N''}$ | $\nu_{1eRN''}$ | $\nu_{2eRN''}$ | $\nu_{1fRN''}$ | $\nu_{4fRN''}$ | $S_{0eN''}$ | $S_{0fN''}$ |
|---|---|---|---|---|---|---|---|---|
| 13 | 26167.0 | 26166.7 | 23628.2 | 23634.5 | 23628.4 | 23635.2 | 8.815 | 8.237 |
| 14 | 26583.7 | 26583.3 | 23662.8 | 23670.0 | 23662.8 | 23670.5 | 9.311 | 8.739 |
| 15 | 27025.1 | 27024.7 | 23697.3 | 23705.4 | 23697.1 | 23705.8 | 9.808 | 9.240 |
| 16 | 27490.8 | 27490.4 | 23731.5 | 23740.7 | 23731.3 | 23741.0 | 10.305 | 9.741 |
| 17 | 27980.1 | 27979.6 | 23765.6 | 23775.8 | 23765.2 | 23776.0 | 10.802 | 10.242 |
| 18 | 28492.4 | 28491.9 | 23799.4 | 23810.6 | 23798.9 | 23810.7 | 11.299 | 10.742 |
| 19 | 29027.1 | 29026.5 | 23832.7 | 23845.0 | 23832.1 | 23845.0 | 11.797 | 11.243 |

**Table 2.** Intensity integral of the $R$ and $Q$ branches in the spectrum in Fig. 2(b).

| $\nu''$ | $A_i$ | $N''$ | $\lambda_1$, $\lambda_2$ (nm) | $\int_{\lambda_1}^{\lambda_2} I d\lambda$ |
|---|---|---|---|---|
| 0 | 1.0000 | 13 | 423.00, 423.35 | 3.54790 |
| 0 | 1.0000 | 14 | 422.39, 422.70 | 3.05579 |
| 0 | 1.0000 | 15 | 421.70, 422.20 | 2.97194 |
| 0 | 1.0000 | 16 | 421.20, 421.50 | 2.23375 |
| 0 | 1.0000 | 17 | 420.60, 421.05 | 2.07326 |
| 0 | 1.0000 | 18 | 419.90, 420.40 | 1.65971 |
| 0 | 1.0000 | 19 | 419.30, 419.90 | 1.32067 |
| 2 | 0.8383 | $\sum_{N''=2}^{22} Q(N'')$ | 432.30, 432.70 | 8.15311 |

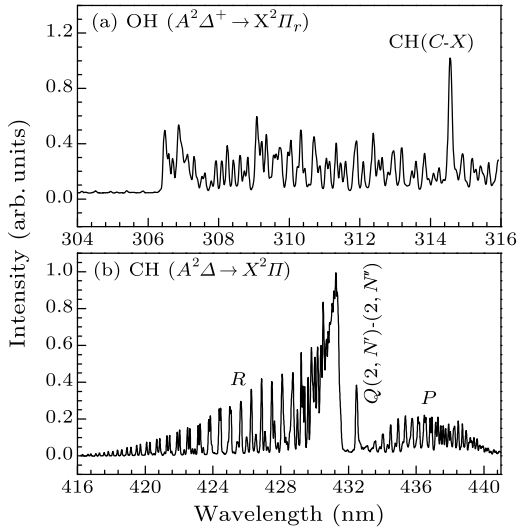


**Fig. 2.** Emission spectroscopy of (a) OH ($A^2\Sigma^+ \rightarrow X^2\Pi_r$) and (b) CH ($A^2\Delta \rightarrow X^2\Pi$) at the inner core of an acetylene-oxygen flame at a rich oxygen state.

A zoomed image of the part of Fig. 2(b) from 418 nm to 428 nm is shown in Fig. 3 to reveal the $R$ branch of the $A^2\Delta(0, N') \rightarrow X^2\Pi(0, N'')$ band of the ES clearly. The ES in Fig. 3 shows the values of the intensity integrals. The intensity integrals of the wavelength ranging from $N'' = 13$ to $N'' = 19$ are calculated and listed in Table 2. The measured results of the $Q$ branch of $A^2\Delta(2, N') \rightarrow X^2\Pi(2, N'')$ are also provided. Figure 4 shows the plots of the $R$ branch from $N'' = 13$ to $N'' = 19$ by using Eq. (3) and the slope of the line by fitting these points, which corresponds to the reciprocal of $T_r = 3141$ K. This result is close to the value of 3342 K at the stoichiometric ratio of the oxygen and acetylene. The latter is solved by the Gaseq software, which is available in the website of www.gaseq.co.uk.

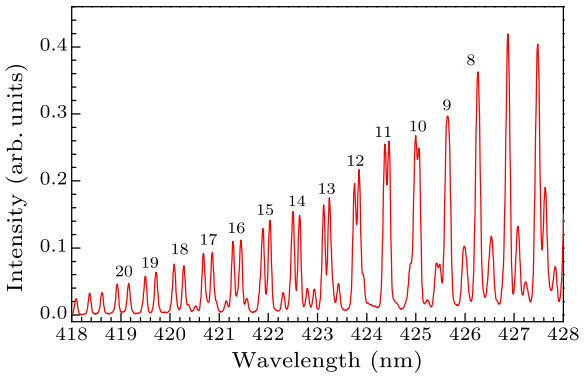


**Fig. 3.** Amplified spectral profile in Fig. 2(b).

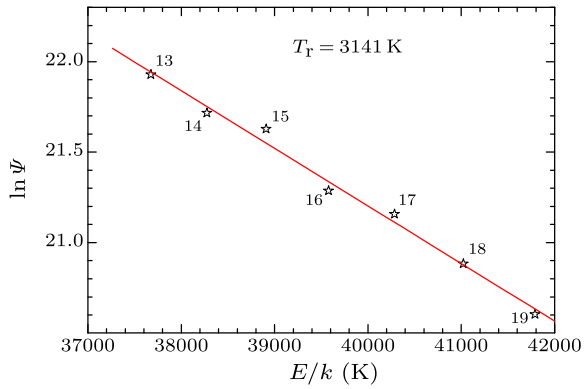


**Fig. 4.** Boltzmann plots of Eq. (3) for CH($A^2\Delta A^2\Delta \rightarrow X^2\Pi$) in Fig. 3. $\Psi = \left[\int I(N'', \lambda) d\lambda\right] \left[S_{0,1,N''}\left(\nu^4_{0,11ee} + \nu^4_{0,11ff}\right) + S_{0,2,N''}\left(\nu^4_{0,22ee} + \nu^4_{0,22ff}\right)\right]^{-1}$.

The peak at 432.4 nm in Fig. 2(b) comes from the radiation of the $Q$ main branches of $\nu'' = 2$. The parameters of the lines of the $Q$ main branch of $2 \leq N'' \leq 22$ can be calculated using the combination relations in Ref. [15]. The calculations are listed in Table 3 for the calculation of $T_\nu$ where the lines of $N'' > 22$ are ignored because they have a low spectral intensity and their wavelengths are also away from 432.4 nm, as shown in Fig. 1.

**Table 3.** Parameters of some rotational lines of Q branch with $\nu'' = 2$ from[13,14]

| $N''$ | $E^e_{2N''}$ | $E^f_{2N''}$ | $v_{1eQN''}$ | $v_{2eQN''}$ | $v_{1fQN''}$ | $v_{2fQN''}$ | $S_{2eN''}$ | $S_{2fN''}$ |
|---|---|---|---|---|---|---|---|---|
| 2 | 28539.1 | 28540.8 | 23118.3 | 23118.2 | 23125.7 | 23125.5 | 1.718 | 0.847 |
| 3 | 28618.3 | 28619.4 | 23119.5 | 23119.2 | 23124.5 | 23124.0 | 3.061 | 2.052 |
| 4 | 28723.5 | 28724.2 | 23120.5 | 23119.8 | 23124.2 | 23123.4 | 4.261 | 3.249 |
| 5 | 28854.6 | 28855.2 | 23121.3 | 23120.4 | 23124.3 | 23123.1 | 5.391 | 4.381 |
| 6 | 29011.4 | 29011.9 | 23122.2 | 23120.8 | 23124.5 | 23123.0 | 6.483 | 5.474 |
| 7 | 29193.8 | 29194.1 | 23123.0 | 23121.1 | 23124.9 | 23122.9 | 7.550 | 6.544 |
| 8 | 29401.4 | 29401.6 | 23123.6 | 23121.3 | 23125.3 | 23122.7 | 8.602 | 7.597 |
| 9 | 29634.0 | 29634.1 | 23124.2 | 23121.3 | 23125.6 | 23122.4 | 9.644 | 8.639 |
| 10 | 29891.1 | 29891.1 | 23124.6 | 23121.0 | 23125.7 | 23121.8 | 10.677 | 9.673 |
| 11 | 30172.3 | 30172.3 | 23124.7 | 23120.4 | 23125.7 | 23121.0 | 11.705 | 10.702 |
| 12 | 30477.3 | 30477.2 | 23124.5 | 23119.4 | 23125.3 | 23119.9 | 12.728 | 11.726 |
| 13 | 30805.5 | 30805.4 | 23123.9 | 23118.0 | 23124.5 | 23118.3 | 13.748 | 12.746 |
| 14 | 31156.5 | 31156.3 | 23122.7 | 23116.0 | 23123.2 | 23116.1 | 14.765 | 13.763 |
| 15 | 31529.6 | 31529.3 | 23120.8 | 23113.2 | 23121.2 | 23113.2 | 15.780 | 14.779 |
| 16 | 31924.2 | 31923.9 | 23118.2 | 23109.7 | 23118.4 | 23109.5 | 16.794 | 15.792 |
| 17 | 32339.8 | 32339.4 | 23114.6 | 23105.2 | 23114.7 | 23104.9 | 17.805 | 16.804 |
| 18 | 32775.7 | 32775.2 | 23109.9 | 23099.5 | 23110.0 | 23099.1 | 18.816 | 17.815 |
| 19 | 33230.9 | 33230.5 | 23104.0 | 23092.6 | 23103.9 | 23092.1 | 19.825 | 18.824 |
| 20 | 33705.0 | 33704.5 | 23096.6 | 23084.2 | 23096.4 | 23083.5 | 20.834 | 19.833 |
| 21 | 34197.0 | 34196.5 | 23087.5 | 23074.0 | 23087.2 | 23073.3 | 21.841 | 20.841 |
| 22 | 34706.1 | 34705.6 | 23076.5 | 23062.0 | 23076.1 | 23061.1 | 22.848 | 21.848 |

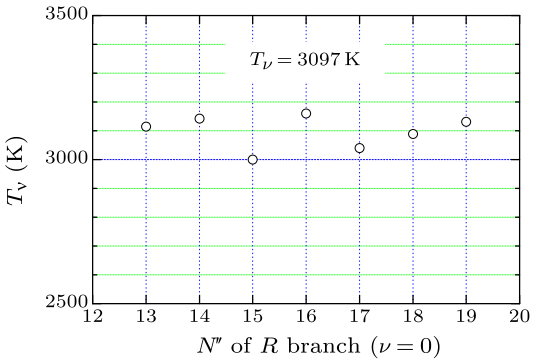


**Fig. 5.** The values of $T_\nu$ deduced by the $R$ branch of $N'' = 13$–$19$ and $\nu'' = 0$ with the $Q$ branch of $\nu'' = 2$.

Considering that the difference of the wave numbers between the states of $A^2\Delta(2,0)$ and $A^2\Delta(0,0)$ is $5287.3\,\mathrm{cm}^{-1}$ and the corresponding temperature value is 7613 K and employing the parameters and the measured results listed in Tables 2 and 3 in Eq. (2), we obtain

$$\int_{\lambda_1}^{\lambda_2} I_Q d\lambda = CA_2 \sum_{N''=2}^{22} \Big[ S_{2eN''}(\nu^4_{1eQN''} + \nu^4_{2eQN''}) \cdot e^{-E^e_{2N''}/kT_\mathrm{r}} + S_{2fN''}(\nu^4_{1fQN''} + \nu^4_{2fQN''}) \cdot e^{-E^f_{2N''}/kT_\mathrm{r}} \Big] e^{-7613/T_\nu}, \quad (4)$$

where the lines of $\nu_{1eQN''}$ and $\nu_{2eQN''}$ have the identical Hönl–London factor and so do those of $\nu_{1fQN''}$ and $\nu_{2fQN''}$. At $T_\mathrm{r} = 3141$ K, combining with Eq. (3) for the lines of the $R$ branch from $N'' = 13$–$19$, the values of $T_\nu$ versus $N''$ are plotted in Fig. 5 and the corresponding average value is 3097 K. The thermal equilibrium between the vibration state and the rotation state is reached because of $T_\mathrm{r} \approx T_\nu$. At the states with temperatures of 3141 K and 3097 K, the ratios of acetylene to oxygen are 2:9.2 and 2:10.2, respectively, which are obtained using the software from www.gaseq.co.uk. They are also in agreement with the ratio of the flux of acetylene to that of oxygen.

In summary, an improved Boltzmann plot method was proposed to determine the rotational and vibrational temperatures. In the method, the intensities of the rotational lines are taken as the integral of the spectral intensity in some special band. The values of the temperatures at the inner core of an acetylene oxygen flame at oxygen-rich conditions are estimated from the data of the experimental spectrum of CH ($A^2\Delta \rightarrow X^2\Pi$). The experimental result reveals that the rotational temperature is equal to the vibrational temperature.

## References


[1] Kim J S and Cappell, M A 1998 *J. Appl. Phys.* **84** 4595
[2] Dermeval C Jr et al 2008 *J. Brail. Chem. Soc.* **19** 1326
[3] Moon S Y et al 2008 *Phys. Plasmas* **15** 103504
[4] Brennen W and Tucker C 1967 *J. Chem. Phys.* **46** 19677
[5] Lago V et al 1996 *27th AIAA Plasma Dynamics Lasers Conference* (New Orleans LA, 17–20 June 1996)
[6] Ndiaye A A and Lago V 2011 *Plasma Sources Sci. Technol.* **20** 015015
[7] Kim S J, Brown M and Spinrad H 1997 *J. Geomagn. Geoelectron.* **49** 1165
[8] Lyddon T D 1968 *Combust. Flame* **12** 541
[9] Yang D et al 2001 *Spectrosc. Lett.* **34** 109
[10] Coitout H and Faure G 1996 *Spectrosc. Lett.* **29** 1201
[11] Pellerin S et al 1996 *J. Phys. D: Appl. Phys.* **29** 726
[12] Charles de lzarra 2000 *J. Phys. D: Appl. Phys.* **33** 1697
[13] Zachwieja M 1995 *J. Mol. Spectrosc.* **170** 285
[14] http://www.sri.com/cem/lifbase
[15] Dieke G H and Crosswhite H M 1961 *J. Quant. Spectrosc. Rad.* **2** 97